MEF2C Hypofunction in Neuronal and Neuroimmune Populations Produces MEF2C Haploinsufficiency Syndrome-Like Behaviors in Mice

Supplement 1

Supplemental Table S1: Summary of Clinical Features of MCHS Patients.

Overview of Clinical Characteristics associated with *MEF2C* variants						
	Newly described				**Previously described (Zweier *et al.* 2010)**	
Demographics						
Sex	F	F	F		F	F
Age at evaluation	13y11m	17m	4y3m		10y5m	3y
Molecular findings						
MEF2C variant	c.120_125dup	c.90G>T	c.137T>C		c.80G>C	c.113T>A
	p.D40_C41dup	p.K30N	p.I46T		p.G27A	p.L38Q
Inheritance of variant	Paternal (father mosaic)	*de novo*	Non-maternal		*de novo*	*de novo*
Clinical findings						
Height (percentile)	23rd	10-25th	25th		25-50th	NR
Weight (percentile)	25th	25-50th	40th		50th	25th
OFC (percentile)	NR	10-25th	25th		50th	9th
Seizures	Yes	Yes	Yes		Yes	Yes
Age of onset	8y	6m	21m		6m	10m
Global developmental delay	Yes	Yes	Yes		Yes	Yes
Speech	Few words	Absent	Few words		Absent	Absent
Tremors/tremulous	Yes	No	No		NR	NR
Hypotonia	Yes (resolved)	Yes	No		Yes	Yes
Brain MRI	Abnormal	Abnormal	Normal		Abnormal	Abnormal
Abnormalities noted	Areas of heterotopia in left lateral region, subtle but progressive abnormalities of white matter within frontal and parietal regions	Asymmetric appearance of hippocampi, asymmetric enlargement of temporal horn of left lateral ventricle	-		Mild under-myelination of insular cortices bilaterally	Generalized lack of white matter bulk and delay in myelin maturation
Repetitive movements	Yes	No	Yes		NR	NR
Breathing abnormalities	Yes	Yes	NR		Yes	No
Jugular fossa pit on anterior neck	No	No	No		NR	NR
High pain tolerance	Yes	NR	Yes		NR	NR

Sleeping difficulties	Yes	No	No		NR	NR
Social abnormalities	No	Yes	NR		NR	NR
Anxiety	No	No	NR		NR	NR
Autism spectrum disorder	No	No	Yes		NR	No
Dysmorphic Findings						
Midface	Hypoplastic	Full cheeks	Normal		NR	NR
Palpebral fissures	Upslanted	Upslanted with epicanthal folds	Normal		Downslanted	Upslanted
Nose	Sharp nasal tip, hypoplastic alae nasi, prominent columella	Normal	Normal		NR	NR
Mouth	Small	Bowed upper lip, small mandible	Dental crowding		Dental crowding, full upper lip	Bowed upper lip, widely spaced teeth
Chest	Mild pectus excavatum	Normal	Normal		NR	NR
Back	Mild lordosis	Normal	Normal		NR	NR
Digits	Long, increased space between toes 1 and 2	Normal	Normal		NR	NR
Other	-	Thin hair	-		Thick hair, large ears, fleshy ear lobes	Large ears, prominent ear lobes

NR=Not Reported

Supplemental Table S2. RNA-Seq gene expression in control and *Mef2c*-Het cortex. See separate Excel file.

Supplemental Table S3. *Mef2c* DEGs compared to single-cell RNA-Seq gene databases. See separate Excel file.

Supplemental Table S4. Primers for qPCR analysis of *Mef2c*-Het DEGs

Gene:	Forward Primer:	Reverse Primer:
Mef2c	GTCGGCTCAGTCATTGGCTAC	CGCTACTCAGAGAGTACTCAG
Mef2c Exon 2	GTGCTGTGCGACTGTGAGAT	CTCCACAATGTCTGAGTTTGTC
Met	GTGAACATGAAGTATCAGCTCCC	TGTAGTTTGTGGCTCCGAGAT
Htr7	TGGGCTATGCAAACTCTCTC	CAGCACAAACTCGGATCTCT
Ntng1	TGCTAAACACAGTCATTTGCGT	TGTTGTTCCAGTCTTACACTCAC
Syt17	GTCAGAGGTGCTATGAGTCCA	GGGGTCAAAGGAACATCGCT
Scn7a	TGTCTCCTCTAAACTCCCTCAG	TGCGTAAATCCCAAGCAAAGT
Gria1	CAAGTTTTCCCGTTGACACATC	CGGCTGTATCCAAGACTCTCTG
Mapk12	AGCCCTCAGGCTGTGAATCT	CATATTTCTGGGCCTTGGGT
Galnt14	GAATGTCTACCCAGAACTCAGGG	CCTTGGCACAGGGACTTAGC
Drd1	TGGCACAAGGCAAAACCTACA	CTGCTCAACCTCGTGTCACA
Htr1b	CGCCGACGGCTACATTTAC	TAGCTTCCGGGTCCGATACA
Wdfy4	AAGTCAGTGTATGTGCTCACG	CTGCCCTTGAACATCGCTCT
C4b	GACAAGGCACCTTCAGAACC	CAGCAGCTTAGTCAGGGTTACA
Slc2a5	TCTCTTCCAACGTGGTCCCTA	GAGACTCCGAAGGCCAAACAG
Stab1	GGCAGACGGTACGGTCTAAAC	AGCGGCAGTCCAGAAGTATCT
C1qc	ACACATCGCATACGGCCAA	AACATGTGGTCGCAGAAGCTG
C1qb	TCACCAACGCGAACGAGAA	AAGTAGTAGAGGCCAGGCACCTT
Ctss	ATAAGATGGCTGTTTTGGATG	TTCTTTTCCCAGATGAGACGC
Spp1	AGCAAGAAACTCTTCCAAGCAA	GTGAGATTCGTCAGATTCATCCG
Slc23a3	TCTTCAACTTCAACTCACAT	ACAAAGGCAGAGATGAAC
Adcyap1	ACCATGTGTAGCGGAGCAAG	CTGGTCGTAAGCCTCGTCT
Islr2	GGCCACTGCGCCTACTCTATCT	GTCCCCCTGCTCCACATCTTCA
Ksr1	GCACCAAGTGCTCAGTGTCTA	CTGAAGCGTGGGTAGCTGTT
Prss23	GGTGAGTCCCTACACCGTTC	GGCGTCGAAGTCTGCCTTAG
Aif1	GTCCTTGAAGCGAATGCTGG	CATTCTCAAGATGGCAGATC
Cd68	CCACAGGCAGCACAGTGGACA	TCCACAGCAGAAGCTTTGGCCC
Il6	TACCACTTCACAAGTCGGAGGC	CTGCAAGTGCATCATCGTTGTTC
Tnf	GGTGCCTATGTCTCAGCCTCTT	GCCATAGAACTGATGAGAGGGAG
Nos2	GAGACAGGGAAGTCTGAAGCAC	CCAGCAGTAGTTGCTCCTCTTC
Tgfb1	TGATACGCCTGAGTGGCTGTCT	CACAAGAGCAGTGAGCGCTGA
Mrc1	GTTCACCTGGAGTGATGGTTCTC	AGGACATGCCAGGGTCACCTTT
Arg1	CATTGGCTTGCGAGACGTAGAC	GCTGAAGGTCTCTTCCATCACC
Il10	GGCAGAGAACCATGGCCCAGAA	AATCGATGACAGCGCCTCAGCC

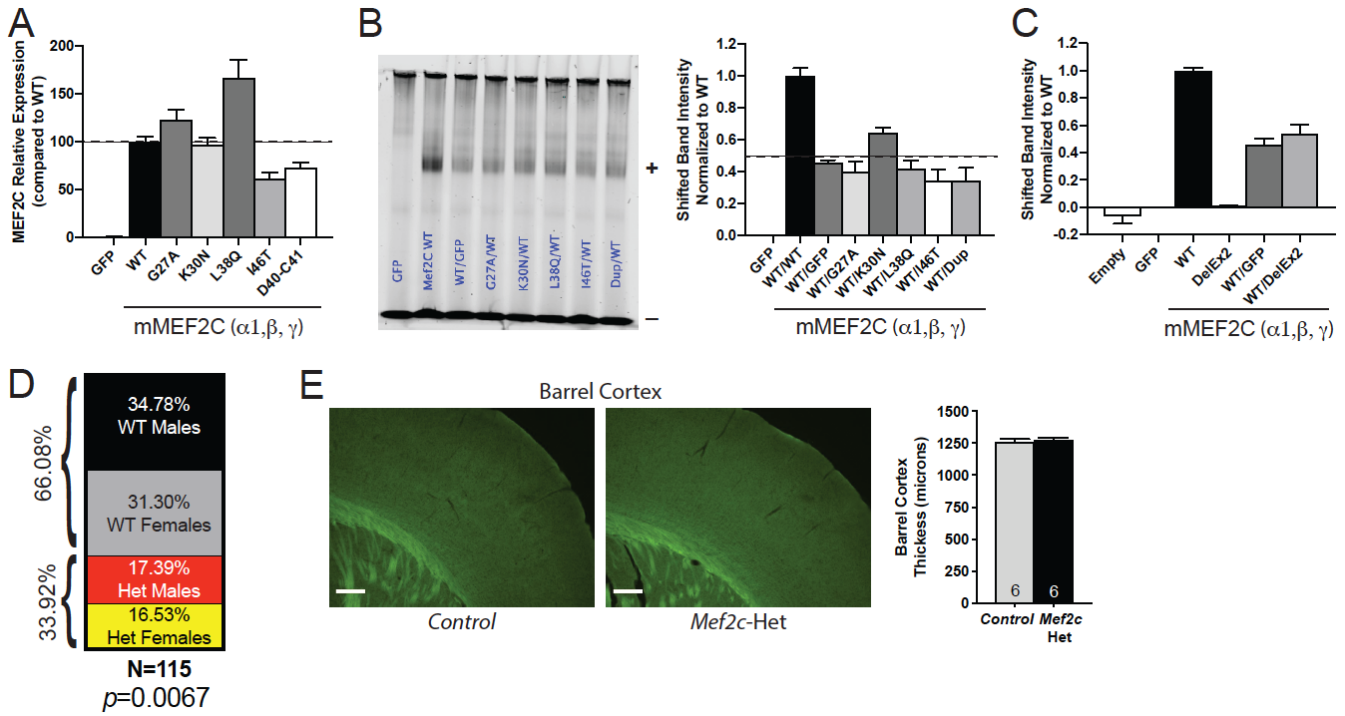

Figure S1. (A) Quantification of MEF2C Western blot from 293-T cells containing MCHS mutations (Fig. 1B). (B) EMSA shows that MCHS-mutations in MEF2C do not disrupt WT MEF2C from binding to the MEF2 response element (MRE). Quantification of MEF2C bound probe is reported (B). (C) Quantification of MEF2C DelEx2 EMSA (Fig. 1F). (D) Genetic distribution of offspring from WT and *Mef2c*-Het mice. (E) Barrel cortical thickness is similar between *Mef2c*-Het and control mice. Scale bar = 250 microns. Data are reported as mean ± SEM. Statistical significance was determined by Chi-squared test (D) or unpaired t-test (E). Number of animals (n) are reported in each graph for respective experiment. Also see Figure 1.

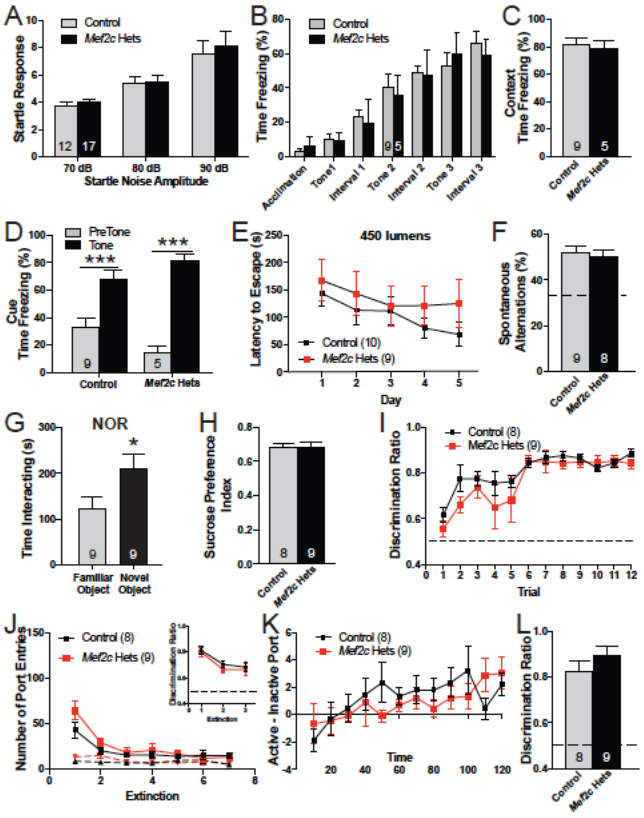

Figure S2. *Mef2c*-Het mice have normal cognitive abilities. (A) There is no difference in acoustic startle response between *Mef2c*-Het and control mice. (B-D) Pavlovian Fear Conditioning. Both control and *Mef2c*-Het mice increase freezing with each tone/shock pairing during training (B) and show similar levels of freezing during the context (C) and cue (D) test. (E) No difference in latency to escape a very bright (450 lumens) Barnes Maze. (F) Both control and *Mef2c*-Het mice have similar spontaneous alternations in the Y-maze. (G) Novel object recognition. *Mef2c*-Het mice (n=9) interacted more with a novel object than a familiar object. (H) Both genotypes show a similar preference for 1% sucrose solution. (I-L) Sucrose Self-Administration Task. (I) Discrimination ratio during sucrose self-administration. (J) Number of active (solid line) and inactive (dashed line) port entries during extinction. Control and *Mef2c*-Het mice can recall the active port on the first day of extinction, and both genotypes show similar extinction rates (J) and discrimination ratio (insert). (K) Discrimination ratio during the first day of sucrose self-administration. (L) Both control and *Mef2c*-Het mice have high discrimination ratios during cue-induced reinstatement of sucrose seeking. Data are reported as mean ± SEM. Statistical significance was determined by 2-way ANOVA (A,B,D,E,I-K) or unpaired t-test (C,F-H,L). *p<0.05, ***p<0.005. Number of animals (n) are reported in each graph for respective experiment. Also see Figure 2.

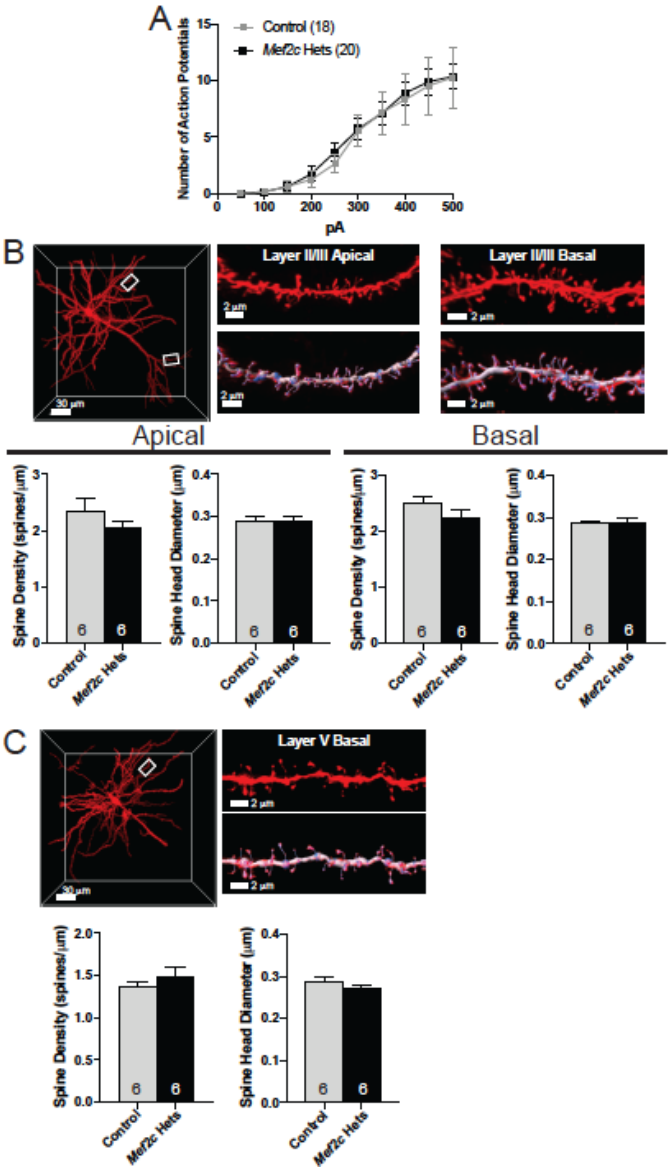

Figure S3. (A) Both control and *Mef2c*-Het cortical pyramidal neurons have similar numbers of action potentials evoked by increasing current injections (500ms, 50pA steps) recorded in current clamp. (B,C) Representative image of a DiI filled cortical pyramidal neuron (B=layer 2/3; C=layer 5) and representative apical and basal dendritic segments used for quantifying dendritic spines. Both control and *Mef2c*-Het mice have similar dendritic spine density and spine head diameter on apical and basal dendrites. Data are reported as mean ± SEM. Statistical significance was determined by 2-way ANOVA (A) or unpaired t-test (B,C). Number of cells (A) or animals (B,C) are reported in each graph for respective experiment. Scale bar=30 μm (neuron) or 2 μm (dendritic stretch). Also see Figure 3.

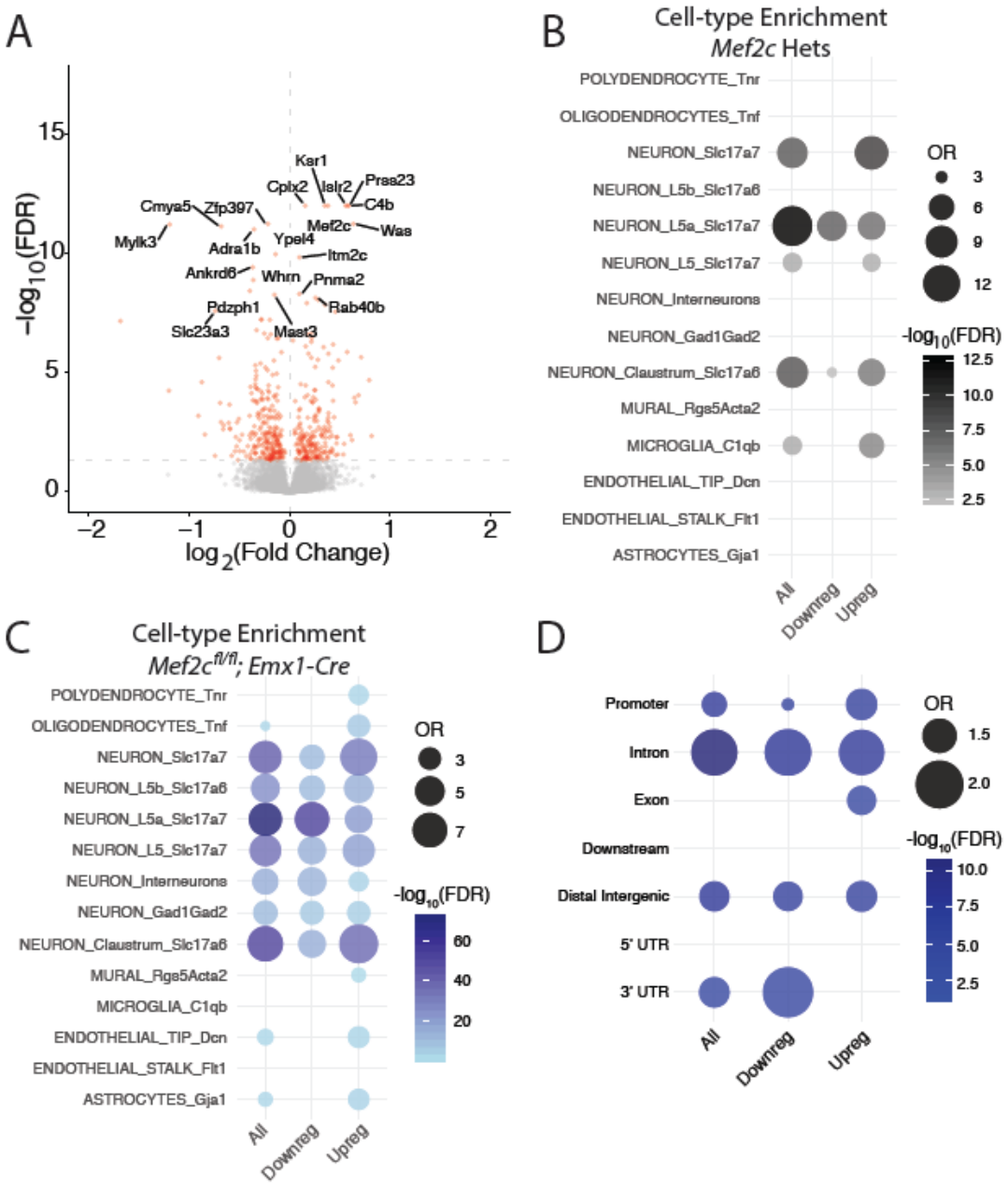

Figure S4. Differentially expressed genes in *Mef2c*-Het cortex. (A) Volcano plot of *Mef2c*-Het DEGs shows genes are both up- and down-regulated in the cortex of *Mef2c*-Het mice. (B) Bubble-plot of *Mef2c*-Het DEGs are enriched for genes expressed in neurons and microglia. (C) Bubble-plot of *Mef2c*-cKO (*Mef2c*$^{fl/fl}$; Emx1-Cre) DEGs show enrichment for neuronal genes but not microglia genes. (D) Bubble-plot of *Mef2c*-Het DEGs compared to genes bound by MEF2C in different genomic regions (MEF2C ChIP). See Methods for statistical tests. Number of animals is 4/genotype. Also see Figure 4.

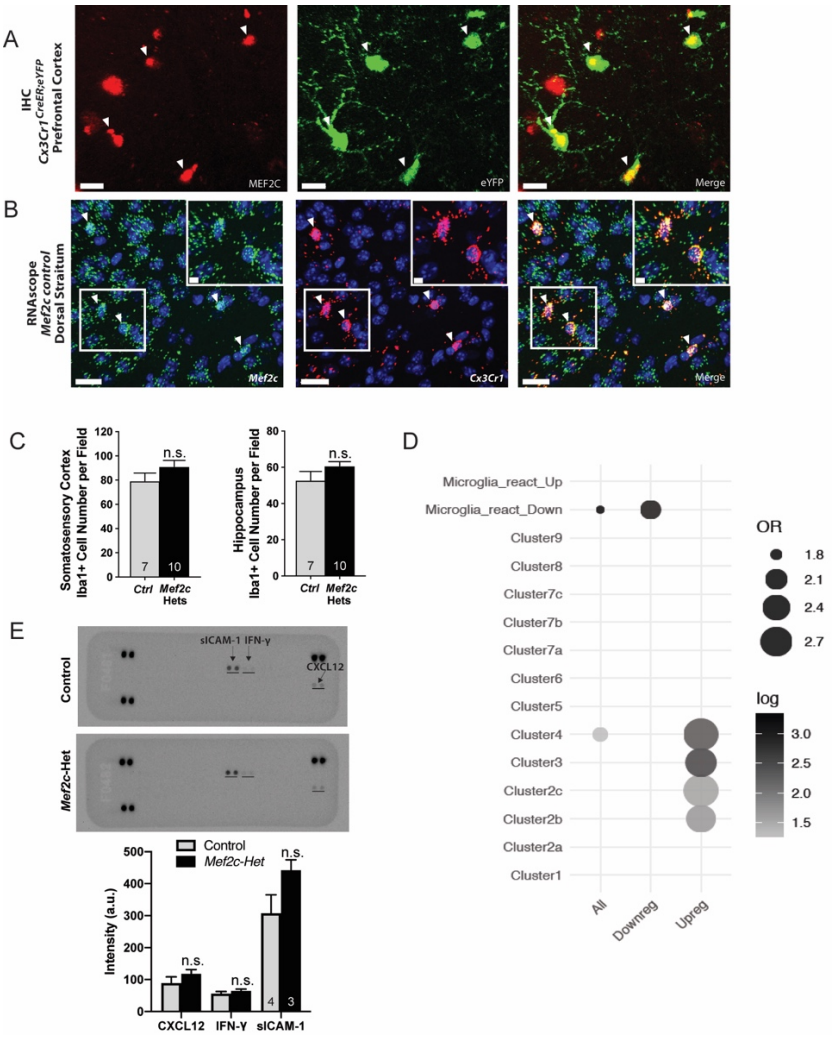

Figure S5. (A) MEF2C is expressed in microglia at the protein level. Using a microglia reporter mouse (*Cx3Cr1*$^{CreER;eYFP}$), immunohistochemistry reveals that MEF2C (red) is expressed in microglia (green) under basal conditions. Scale bar = 10 microns. (B) *Mef2c* is expressed in microglia at the mRNA level. RNAscope against *Mef2c* (green) and *Cx3Cr1* (a microglial marker, in red) demonstrates *Mef2c* mRNA expression in microglia in the dorsal striatum. Scale bar = 20 microns and 5 microns (inset). (C) Microglial cell density in the somatosensory cortex and dentate gyrus of the hippocampus, quantified via Iba1 staining of microglia, is not significantly different between *Mef2c*-Hets and controls. (D) Enrichment of differentially expressed genes in *Mef2c*-Hets are upregulated in cluster 2b (G-phase proliferative cluster), cluster 2c (M-phase proliferative cluster), and cluster 3 (metabolically active microglia at E14.5), and cluster 4 (microglia associated with unmyelinated axon tracts at P4/5). (E) Cytokine antibody array analysis for assessing neuroinflammation in *Mef2c*-Hets and controls at P35-P40. Data are reported as mean ± SEM. Statistical significance was determined by unpaired t-test (C,E). Number of animals (C,E) are reported in each graph for respective experiment. Also see Figure 5.

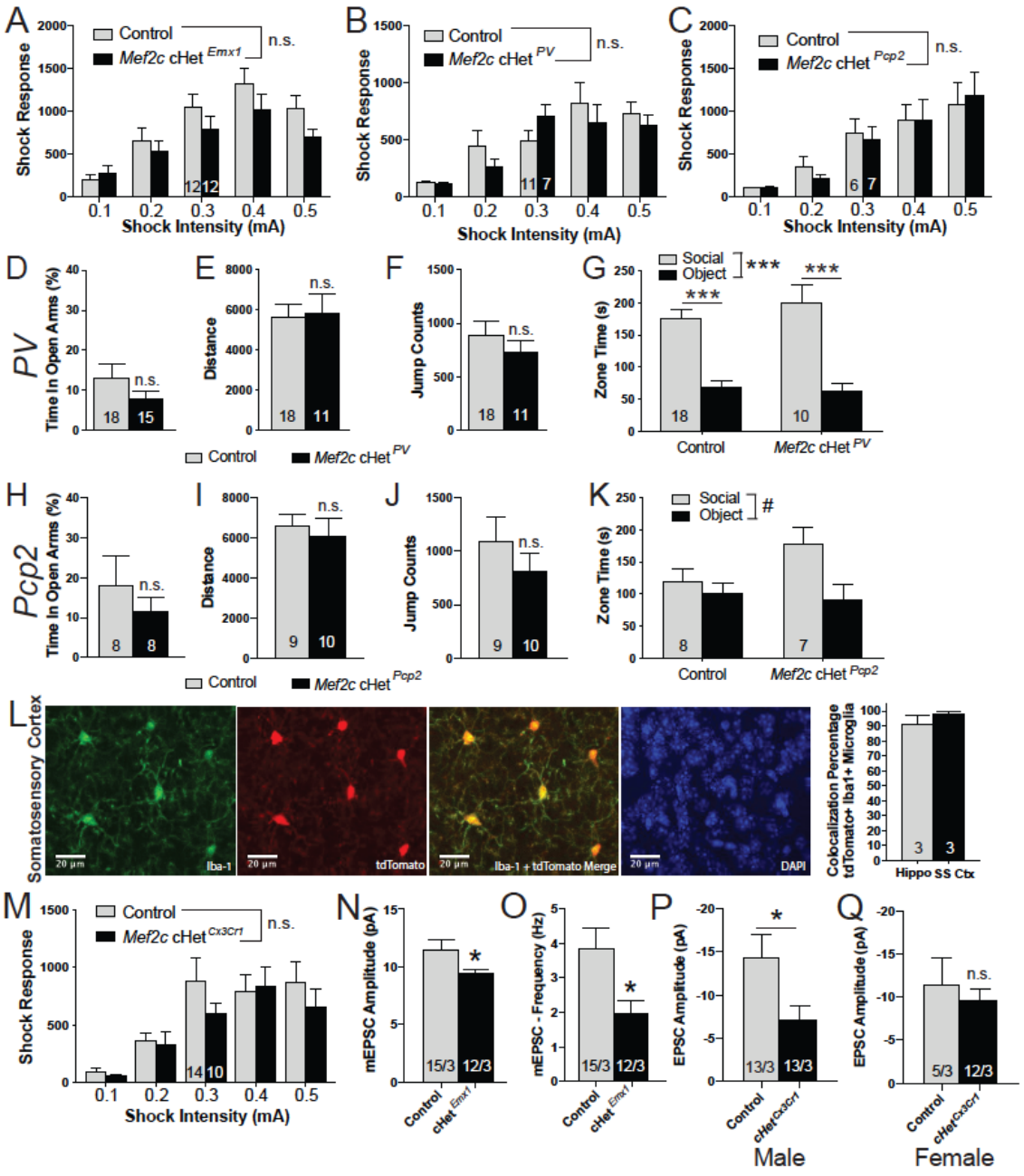

Figure S6. (A-C) *Mef2c* cHet^{Emx1} (A), *Mef2c* cHet^{PV} (B), and *Mef2c* cHet^{Pcp2} (C) mice have normal response to shock. (D-G) Behaviors in *Mef2c* cHet^{PV} mice. (D) *Mef2c* cHet^{PV} mice spend similar time on the open arms of the EPM. (D,E) Male *Mef2c* cHet^{PV} mice have similar activity (E) and jump counts (F). (G) *Mef2c* cHet^{PV} mice have normal social interaction. (H-K) *Mef2c* cHet^{Pcp2} mice are similar to controls in elevated plus maze (H), activity (I), jump counts (J), and social interaction (K). (L) Recombination efficiency after p1-p3 tamoxifen treatment in *Cx3Cr1*$^{CreER;eYFP}$; Ai14 mice. tdTomato expression suggests recombination in these Iba1-postive microglia cells. (M) *Mef2c* cHet^{Cx3Cr1} mice are similar to controls in shock response. (N,O) *Ex vivo* recordings from organotypic slices were collected from pyramidal neurons

within the barrel cortex field of *Mef2c* cHet^{Emx1} mice. Neurons from *Mef2c* cHet^{Emx1} show reduced mEPSC amplitude (N) and frequency (O) compared to controls. (P,Q) *Ex vivo* recordings from organotypic slices were collected from pyramidal neurons within layer 2/3 of the barrel cortex field of *Mef2c* cHet^{Cx3cr1} mice. Male *Mef2c* cHet^{Cx3cr1} mice show reduced evoked EPSC amplitude in layer 2/3 pyramidal neurons in the barrel cortex compared to controls (P). Female *Mef2c* cHet^{Cx3cr1} mice do not have differences in evoked EPSC amplitude compared to controls (Q). Data are reported as mean ± SEM. Statistical significance was determined by 2-way ANOVA (A-C,G,K,M) or unpaired t-test (D-F,H-J,L,N-Q). #$p<0.1$, *$p<0.05$, ***$p<0.005$, n.s. = not significant. Number of animals (A-M) or cells/animals (N-Q), respectively, are reported in each graph for respective experiment. Also see Figure 6.

Supplemental Methods

Patients

Patients with developmental delay and a significant variant in the MEF2C gene were selected for this study. These patients were seen for clinical genetics evaluations and data from these visits were gathered from records review. Internal informed consent to publish data was obtained for each subject.

Animals

Mice (*Mus musculus*) were group housed (2-5 mice/cage; unless specified) with same-sex littermates with access to food and water *ab libitum* on a 12 hour reverse light-dark cycle. *Mef2c*$^{+/-}$ (*Mef2c*-Het) mice were initially generated by crossing *Mef2c*$^{fl/fl}$ (RRID:MGI:3719006)(1) mice with *Prm1-Cre* (Jackson Laboratory #003328) to induce germline recombination of *Mef2c*. *Mef2c*$^{+/-}$*; Prm1-Cre* were crossed with C57BL/6J to remove *Prm1-Cre*, and test mice were generated from *Mef2c*$^{+/-}$ mice crossed with C57BL/6J mice. *Mef2c* conditional het mice were generated by crossing *Mef2c*$^{fl/fl}$ mice with heterozygous cell-type specific Cre mice (*Emx1-Cre* (Jackson Laboratory #005628)(2); *Pcp2-Cre* (Jackson Laboratory #004146)(3); *PV-Cre* (Jackson Laboratory #017320) to generate *Mef2c*$^{fl/+}$; *Cre* conditional heterozygous (*Mef2c* cHet) mice that were compared to their Cre-negative littermates. *Cx3Cr1*-Cre *Mef2c* conditional heterozygous (*Mef2c* cHet^{Cx3Cr1}) mice were generated by crossing *Cx3Cr1*$^{creER/creER}$ males (Jackson Laboratory #021160)(4) with *Mef2c*$^{fl/+}$ females to produce *Cx3Cr1*$^{creER/+}$; *Mef2c*$^{fl/+}$ (experimental) and *Cx3Cr1*$^{creER/+}$; *Mef2c*$^{+/+}$ (control) mice. Experimenters were blinded to the mouse genotype during data acquisition and analysis. Experiments were independently replicated, and the total number of animals/cells were reported in the representative figures. All procedures were conducted in accordance with the Institutional Animal Care and Use Committee (IACUC) and NIH guidelines.

EMSA: Electrophoretic mobility shift assay (EMSA) was performed as previously described (5) with modifications. Briefly, proteins were isolated from 293-T cells 48 hours after transfection of

pA1T7α::*Mef2c* variants in a non-denaturing EMSA cell lysis buffer (20 mM tris-HCl (pH 8.0), 100 mM NaCl, 1 mM EDTA, 1 mM Na_3VO_4, 10 mM NaF, 0.5% Nonidet P-40, 1 μM cyclosporin A, 1X Complete Protease Inhibitor cocktail (Roche)), and quantified using the DC protein assay kit (BioRad). Isolated proteins (10 μg) were incubated with fluorescent-tagged (Infrared Dye 700) Mef2 Response Element (IR700::MRE) probes for 60 minutes at room temperature (RT) and resolved in a non-denaturizing acrylamide gel (50 mM tris-HCl (pH 7.5), 380 mM glycine, 2 mM EDTA, 4% acrylamide/bis-acrylamide (BioRad)). Gels were imaged using the Li-Cor Odyssey CLx, and fluorescence was quantified by Li-Cor Image Studio v3.1.4. Data reported represent the mean from at least 3 biological replicates.

Immunoblotting: EMSA proteins were denatured by adding 4X sample buffer (+DTT, +βME) to samples in EMSA cell lysis buffer and boiling for 10 minutes. Somatosensory cortex was isolated from adult (8 weeks old) male mice and frozen on dry ice. Tissues were sonicated on ice in an SDS lysis buffer (1% (w/v) SDS, 300 mM sucrose, 10 mM NaF (Sigma), 50 mM HEPES (Sigma), and 1X Complete Protease Inhibitor cocktail (Roche)), boiled for 10 minutes, then centrifuges at 16,000 x g for 10 minutes. Total protein concentration was determined by the DC protein assay kit (BioRad). For western blots, 20 μg of total protein was resolved using 10% SDS-PAGE (BioRad). Proteins were transferred to Immobilon-FL PVDF (Millipore), blocked in Odyssey blocking buffer (Li-Cor) for 2 hours, and incubated overnight with either anti-HA (Sigma-Aldrich H6908; 1:2000) and anti-GFP (Aves Labs GFP-1020; 1:2000) for EMSA proteins, or anti-Mef2c (AbCam ab197070; 1:2500) and anti-Neuronal class III β-tubulin (Tuj1, Covance; 1:10,000) antibodies for cortical proteins. Blots were developed with Odyssey CLx Western blot system (Li-Cor Biosciences) (HA, MEF2C, and TUJ1) or ChemiDoc MP Imaging System (BioRad) (GFP).

Data Acquisition: All experiments were independently replicated at least twice (typically 3-4 times). The numbers of animals/neurons/dendritic stretches are reported in each figure, and these numbers were

estimated based on previous reports. Outliers were determined using GraphPad's Outlier calculator (Grubb's) and excluded from data analysis.

Mouse Behavior Testing: For all behavior tests, test mice were acclimated to transport and handling for at least 3 days prior to testing. Before each test, mice were acclimated after transport for >30 minutes prior to testing. Behaviors in *Mef2c*-Het mice were compared to control littermates tested on the same day. All behavioral tests were conducted using young adult mice (8-12 weeks), except juvenile communication (USV) recordings. Both male and female animals were included, except for adult ultrasonic vocalizations recordings. All behavior tests were conducted during the dark-phase (active-phase), and the experimenters were blind to genotypes.

Behavior Data Analysis: All data are presented as mean ± SEM. All comparisons were between littermates using appropriate two-sided statistical tests (specified in figure legends). Normal distribution of the data was assumed. Outliers were determined using GraphPad's outlier calculator (Grubb's) and excluded from analysis. *P*-values were calculated with unpaired *t*-test (two-tailed) or two-way ANOVA followed with Sidak's multiple comparisons post-hoc test using GraphPad Prism, with specific tests described in figure legends.

***Social Interaction*:** Mice were acclimated to the 3-arena sociability apparatus (Stoelting #60450) for 10 minutes. After acclimation, test mice were removed from the arena, and a novel, conspecific mouse and a novel object (medium black paper binder) were placed in a holding chamber within the side arenas. Test mice were returned to the arena and recorded for 10 minutes using ANY-maze behavior tracking software (Stoelting). Time is defined as time spent in each arena.

***Ultrasonic Vocalization Recordings*:** Social ultrasonic vocalizations (USVs) were recorded from adult mice as previously described(6, 7). Briefly, ovariectomized female mice (C57BL/6; Jackson Labs) were

injected with 15-μg estradiol 48 hours prior to testing and 1-mg progesterone 4 hours before testing to induce estrous. Test mice (8-12 week old male mice) were acclimated to a clean home-cage in a sound attenuated chamber for 5 minutes. After acclimation, an estrous female was introduced into the holding chamber with the male test mouse, and USVs were recorded for 5 minutes using Avisoft UltraSoundGate equipment (UltraSoundGate 116Hb with Condenser Microphone CM16; Avisoft Bioacoustics, Germany). USVs were analyzed using Avisoft SASLab Pro (Avisoft Bioacoustics) using a 20 kHz cutoff. ***Distress USVs*** were recorded from juvenile mice (pups) as previously described(6-8). Briefly, individual pups of both sexes were identified with long-lasting subcutaneous tattoos (green tattoo paste; Ketchum) on the paws on post-natal day 4 (P4). Pups of both sexes were recorded in a random order in a small, sound-attenuated chamber following separation from dam and littermates. USVs were recorded for 3 minutes on post-natal days 7 and 10. USVs were quantified using Avisoft SASLab Pro (Avisoft Bioacoustics, German) with experiments blind to genotype.

Rotarod Test**:** Mice were placed on the roller in a Rotarod apparatus (Ugo Basile Apparatus #47600) for a 2-minute training session with a rotation of 4 rpm or 8 rpm and replaced if mouse falls during training session. On the next day, test mice were returned to the roller, and the speed steadily increases from 4-40 rpms over 5 minutes. The latency and rpm for the mouse to fall off the roller were recorded. Each animal receives four testing sessions.

Locomotor Activity**:** Test mice were placed inside the Open Field Activity, Infrared Photobeam Activity Test Chamber (Med Associates), where an array of photobeams measures the mouse's locomotor activity and jumping. Activity was monitored in the dark for one hour, and data are presented as the total activity during the hour.

Elevated Plus Maze (EPM): Mice were introduced in the center of the elevated plus maze (Stoelting #60140) in white light (100 lux) and recorded for 5 minutes using ANY-maze behavior tracking software (Stoelting) with center-point detection. Data are reported as the percent of time spent in the open areas.

***Fear Conditioning Test*:** Fear conditioning was performed as previously described(9). Briefly, test mice were placed in a fear conditioning chamber (Med Associates) and allowed to explore the arena for 2 minutes, after which a loud auditory stimulus (30 secs; 90 dB) that co-terminates with a 2-second mild foot-shock (0.5 mA) was presented to the animal. The mice were exposed to 3 tone/shock pairing with a 1-minute interval separating each tones/shock. The next day, animals were returned to the chamber and behavior (freezing) in the context, in a new context, and with the audible tone played in a new context is recorded with a video-tracking system (Video Freeze V2.7; Med Associates). Data are presented as percent of time the mouse is immobile.

Barnes Maze: Barnes maze was conducted as previously described(10) with modifications. Briefly, on the initial trial, mice were acclimated to the escape chamber for 2 minutes before testing. During testing, mice were introduced to the center of the Barnes Maze (Stoelting #60170) in bright white light (250 or 450 lux) with 4 distinct spatial cues evenly distributed around the arena. Mice were allowed to freely explore the arena for 5 minutes or until the mice found and entered the escape chamber. Latency to escape was recorded for each trial. Mice failing to find the escape chamber at the end of the trial were guided to the escape hole. All mice were left in the escape chamber for 2 minutes before being returned to their home cage. Each mouse was tested twice a day, and data reflect the average latency to enter the escape hole of the 2 trials per day.

Y-maze: Mice were introduced into one arm of a Y-maze (Stoelting #60180) with minimal white light (30 lux), and the mice were video tracked using ANY-maze behavior tracking software (Stoelting) for 5

minutes. Correct alternations were considered when the mouse entered a series of 3 different arms without re-entering a previously explored arm.

Novel Object Recognition (NOR): Mice were acclimated for 10 minutes to an open field arena (OF; 44cm^2) in dim light (30 lux) the day before testing. On test day, mice were acclimated to the OF for 5 minutes before objects were introduced. Mice were presented with 2 identical objects located on opposite sides of the OF arena and allowed to explore the objects for 10 minutes. One initial object was replaced with a novel object, and the mice were allowed to explore the objects for 10 minutes. Mice were recorded and analyzed using ANY-maze behavior tracking software (Stoelting). Interactions were considered when the center of the mouse was within 8 cms from the center of the object.

***Sucrose Preference*:** Test mice were singly housed and provided 2 identical ball-bearing sipper-style bottles to drink. Mice were acclimated to the 2 bottles for 4 days, where both bottles contained water on days 1 and 3 or sucrose solution on days 2 and 4. On days 5-8, mice were presented with 2 bottles, one with water and one with sucrose (1% (w/v)). Daily, the consumption of water and sucrose/quinine was measured, and the bottle position was altered to avoid potential side bias(11). Data is presented as (solution consumption – water consumption) / total consumption = Preference Index.

Sucrose Self-Administration: Sucrose self-administration (SA) was performed as previously described(12). Briefly, mice were introduced to an operant conditioning chamber (Med Associates) at the same time each day during the dark cycle (active-phase). Both a light above the active nose poke hole and the house light indicated that sucrose was available. After an active hole nose poke, the availability lights went off and an internal light in the nose poke hole was activated. Active nose pokes immediately delivered a sucrose pellet (15 mg; TestDiet) and was followed by a 10 s time-out period. Inactive hole nose pokes did not have any consequences. After 12 days of acquiring, the mice entered a 7-day abstinence phase in their home cages and were not exposed to the operant conditioning chamber.

Following abstinence, the mice were placed back in the operant chamber for 2 hours, where the sucrose pellets and cues were not present. Following 7 days of extinction, mice were re-introduced to the operant chamber and the availability cues and reward delivery cue (but no sucrose reward) were presented (cue-induced reinstatement). The number of active and inactive hole nose pokes were recorded during each session. Discrimination ratio is reported as number of active port entries / total number of port entries (active + inactive).

***Shock and Acoustic Startle Response*:** Shock and acoustic startle response was performed as previously described(7). Briefly, shock and startle responses were measured using Startle Reflex System and Advanced Startle software program (Med Associates). Mice were placed in Plexiglas and wire grid animal holders (ENV-264C) attached to a load cell platform (PHM-250) contained within a sound-attenuated chamber. For shock sensitivity, foot shocks (0.1 – 0.5 mA) were delivered by S/A Aversive Stimulators (ENV-414S) connected to the wire grid floors of the animal holder. For acoustic startle, mice were exposed to 5 white-noise pulses/amplitude (38ms) at 3 different amplitudes (70, 80, 90 dB) in a randomized order with variable inter-trial intervals (10-20s). Displacements of the load cell stabilimeter were converted into arbitrary units by an analog-to-digital converter interfaced to a personal computer.

RNA Isolation and Reverse Transcription PCR: Cortical tissue from p35-p40 mice (2 males and 2 females per genotype) were rapidly dissected and frozen at -80˚C. Samples were thawed in TRIzol (Invitrogen), homogenized, and processed using the miRNeasy Mini Kit (Qiagen) according to manufacturer's protocol. Total RNA was reverse-transcribed using Superscript III (Invitrogen) with random hexamers following manufacturer's protocol. Quantitative real-time PCR was performed by the CFX96 qPCR instrument (Bio-Rad) using iTaq Universal SYBR Green Supermix (Bio-Rad) and primers specific to each target gene (Table S4). GAPDH was used to normalize gene expression in each sample.

RNA Sequencing: Total RNA was isolated from whole cortex of p35-p40 mice as described above. Sequencing was performed by BGI Americas Corporation (Cambridge, MA) using polyA mRNA isolation, directional RNA-seq library preparation, and the BGISEQ-500 platform with 150bp paired-end reads using DNA Nanoball (DNB) technology.

RNA-seq Mapping, QC and Expression Quantification: Reads were aligned to the mouse mm10 reference genome using STAR (v2.7.2a) (13) with the following parameters: "*--outFilterMultimapNmax 10 --alignSJoverhangMin 10 --alignSJDBoverhangMin 1 --outFilterMismatchNmax 3 --twopassMode Basic*". For each sample, a BAM file including mapped and unmapped reads that spanned splice junctions was produced. Secondary alignment and multi-mapped reads were further removed using in-house scripts. Only uniquely mapped reads were retained for further analyses. Quality control metrics were performed using RseqQC using the m10 gene model provided. These steps include: number of reads after multiple-step filtering, ribosomal RNA reads depletion, and defining reads mapped to exons, UTRs, and intronic regions. Picard tool was implemented to refine the QC metrics (http://broadinstitute.github.io/picard/). Genecode annotation for mm10 (version M21) was used as reference alignment annotation and downstream quantification. Gene level expression was calculated using HTseq (v0.9.1) using intersection-strict mode by gene (14). Counts were calculated based on protein-coding genes from the annotation file.

Differential Expression: Counts were normalized using counts per million reads (CPM). Genes with no reads in either *Mef2c*-Het or WT samples were removed. Differential expression analysis was performed in R using linear modeling as following: *lm(gene expression ~ Treatment)*

Fitting this model, we estimated $\log_2$ fold changes and P-values. P-values were adjusted for multiple comparisons using a Benjamini-Hochberg correction (FDR). Differentially expressed genes where consider for FDR < 0.05.

Functional Enrichment. The functional annotation of differentially expressed and co-expressed genes was performed using ToppGene (15). We used GO and KEGG databases. Pathways containing between 5 and 2000 genes were retained. A Benjamini-Hochberg FDR ($P < 0.05$) was applied as a multiple comparisons adjustment.

***Gene Set Enrichment*:** Gene set enrichment was performed using a Fisher's exact test in R with the following parameters: alternative = "greater", conf.level = 0.95. We reported Odds Ratios (OR) and Benjamini-Hochberg adjusted P-value (FDR).

ChIP-seq Analysis: FASTQ-files for ChIP-seq were processed following the official ENCODE guidelines (https://github.com/ENCODE-DCC/chip-seq-pipeline2). MEF2C ChIP-seq (16) reads were aligned to the mouse mm10 reference genome using BWA (v0.7.16a)(17). Reads were filtered for MAPQ > 10 and duplicates were removed using samtools (v1.3.1)(18). Quality metrices were inferred using SPP(19) and picard (http://broadinstitute.github.io/picard/). MACS2 (v2.1.1)(20) was used to identify significant peaks using input DNA without ChIP as reference. Peak annotation and visualizations were done in R using Chipseeker library(21).

Availability of Data and Material: The NCBI Gene Expression Omnibus (GEO) accession number is GSE139419 (token: ibkpqcuktjmlvan)**.**

Code Availability: Custom R codes and data to support the analysis, visualizations, functional and gene set enrichments are available at https://github.com/konopkalab/Mef2c_Het.

Barrel Cortex Immunohistochemistry: Mice were transcardially perfused with 1X PBS followed by 4% paraformaldehyde (PFA) in PBS. Brains were hemisected and cortex was isolated. Cortices were flattened between 2 glass slides and post-fixed in 4% PFA for >24 hours. Cortices were cryoprotected in

sucrose then sliced on a sliding stage microtome at 40 μM. Slices were blocked with 5% normal donkey serum and 1% albumin from bovine serum (0.3% TritonX-100, 1X PBS) for 2 hours, incubated with primary antibody anti-vGLUT2 (Abcam ab79157; 1:500) for overnight, incubated with Cy3 conjugated secondary antibody, and dehydrated. Cover slips were mounted using DPX mountant (Sigma).

Cortical Thickness: To assess cortical thickness of *Mef2c*-Het and control mice, 40 μm brain sections at the level of the caudal barrel cortex (approximately bregma -0.22 mm to bregma -0.82 mm) were stained using the BrainStain Imaging kit (ThermoFisher #B34650, FluoroMyelin, 1:300). Three to four FluoroMyelin images were taken per brain region using a 4X objective on a Nikon Eclipse 80i upright epifluorescence microscope connected to a Prior Lumen 200 UV illumination source. Cortical thickness was measured using ImageJ software (NIH).

Electrophysiology: All acute-slice electrophysiological experiments were performed in control and *Mef2c*-het mice at ages P30-P40. Acute coronal slices (300-μm thickness) containing barrel cortex were prepared in a semi-frozen 300 mOsM dissection solution containing (in mM): 100.0 choline chloride, 2.5 KCl, 1.25 Na2H2PO4, 25.0 NaHCO3, 25.0 D-glucose, 3.1 Na pyruvate, 9 Na ascorbate, 7.0 MgCl2, 0.5 CaCl2 and 5.0 kynurenic acid and was continually equilibrated with 95% O2 and 5% CO2 prior to and during the slicing procedure. Slices were transferred to a 315 mOsM normal artificial cerebrospinal fluid (ACSF) solution containing (in mM): 127 NaCl, 2.5 KCl, 1.20 Na2H2PO4, 24 NaHCO3, 11 D-glucose, 1.20 MgCl2, and 2 2.40 CaCl2, 0.4 Na Ascorbate to recover at 37°C for 30 minutes, and then transferred to room temperature ACSF for an additional 30 minutes prior to recording.

Layer 2/3 (L2/3) pyramidal neurons (depth 30-100 μm into the slice) of barrel cortex were visualized with infrared differential interference contrast optics (DIC/infrared optics) and identified by their location, apical dendrites, and burst spiking patterns in response to depolarizing current injection. Unless stated otherwise, all electrophysiological experiments were performed in whole cell voltage clamp mode at -70

mV using borosilicate pipettes (4-6 MΩ) made on NARISHIGE puller (NARISHIGE, PG10) from borosilicate tubing (Sutter Instruments) and filled by an internal solution containing (in mM): 120 K-Gluconate, 5 NaCl, 10 HEPES, 1.1 EGTA, 4 MgATP, 0.4 Na2GTP, 15 phosphocreatine, 2 MgCl2, and 0.1 CaCl2.

All data (Recordings) were acquired and analyzed by amplifier AXOPATCH 200B (Axon Instruments), digitizer BNC2090 (X National instruments) and software AxoGraph v.1.7.0, Clampfit v 8.0 (pClamp, Molecular devices) and Mini Analysis Program v.6.0.9 (Synaptosoft). Data were filtered at 2 kHz by AXOPATCH 200B amplifier (Axon Instruments) and digitized at 10-20 kHz via AxoGraph v.1.7.0.

Evoked Postsynaptic Currents: The evoked postsynaptic responses of BC pyramidal neurons in L2/3 were elicited by field stimulation of excitatory afferents in L4 directly underneath the recorded cells or in L2/3 of the adjustment barrel column at frequency of 0.05 Hz (0.05 c^{-1}) - 3 stimulus in one second. The low-intensity pulses of stimulated current (25–100 mkA, 50–100 mks duration) were applied through a fine-tipped (~2 mkm), bipolar stimulating electrode made from the borosilicate theta glass capillary tubing.

AMPA-receptor-mediated excitatory postsynaptic currents (EPSCs) were recorded in presence of picrotoxin (100 mkM, Sigma Aldrich) to block $GABA_A$Rs. Inhibitory postsynaptic currents (IPSCs) mediated by $GABA_A$ receptors were recorded in presence of DNQX (20 mkM, Tocris) to eliminate the current through AMPA-receptors. Outliers were assessed by ROUT test in Graphpad Prism software and excluded from analysis.

For Paired-Pulse Ratio (PPR) measurements, two EPSC amplitudes were generated at -70mV with the inter-stimulus interval of 50 msec. The peak amplitude of the second EPSC (P2) was divided by the peak of the first amplitude (P1) to generate the PPR ratio (P2/P1).

Miniature Postsynaptic Current: Excitatory (E) and inhibitory (I) miniature postsynaptic currents (mPSCs) were recorded from L2/3 pyramidal neurons in voltage clamp mode at -70 mV. Pyramidal

neurons were identified by their morphology parameters (pyramidal shape of soma, apical dendrite) and by bursting pattern of action potentials firing in response to depolarizing current injection. After identification, the normal ACSF was replaced by solution for mPSCs-records. For mEPSCs mediated by AMPARs, the extracellular bath solution (ACSF) contained 1 μM tetrodotoxin (TTX, Fisher Scientific) and 100 μM pictrotoxin (Sigma Aldrich). mIPSCs were recorded using a high-chloride internal solution with a reversal potential at ECl- = -15 mV for chloride containing (in mM): 79 (70) K-gluconate, 44 (75) KCl, 6(2) NaCl, 10(11) HEPES, 0.2 EGTA, 4(2) MgATP, 0.4 (0.2) Na2GTP, 2 (1) MgCl2, and 0.1 CaCl2. For record $GABA_A$Rs-mediated mIPSC the extracellular bath solution (ACSF) contained 1 μM TTX and 20 μM DNQX (AMPA-receptor antagonist, Tocris). For recording AMPARs-mediated mEPSC the extracellular bath solution (ACSF) contained 1 μM TTX and 100 μM picrotoxin ($GABA_A$Rs antagonist, Sigma-Aldrich).

At the beginning of each sweep, a depolarizing step (4 mV for 100 ms) was generated to monitor series (10-40 MΩ) and input resistance (>400 MΩ). Data were collected in a series of traces until >300 events were recorded. Synaptic events were detected via custom parameters in MiniAnalysis software (Synaptosoft, Decatur, GA) and subsequently confirmed by observer. For each event, amplitude and frequency was measured and used to determine average mean.

Dendritic Spine Analysis: Dendritic spine labeling was done as previously described(22) with some modifications. Briefly, mice were lightly transcardially perfused with 1.5% PFA in PBS and brains were post-fixed for 1 hour at 4°C in 1.5% PFA. Brains were sectioned at 200 μm using a vibrating microtome (Leica VT100P). Tungsten particles (1.3 μm diameter; Bio-Rad) were coated with lipophilic carbocyanine dye DiI (Life Technologies) and diolistically delivered into cortical regions using a Helios Gene Gun system (Bio-Rad) fitted with a polycarbonate filter (3.0 μm pore size; BD Biosciences). After delivering the DiI-coated particles, slices were incubated in PBS at 4°C overnight to allow the dye to diffuse along the neuronal dendrites and axons, then post-fixed for 1 hour in 4% PFA before mounting with Prolong® Gold Antifade (Invitrogen) and imaging. Images of secondary and tertiary L2/3 apical (4-7 segments per

animal, 31 segments per group) and tertiary basal dendrites (3-7 segments per animal, WT=31 segments, het=26 segments) and L5 tertiary basal dendrites (3-5 segments per animal, WT=23 segments, het=21 segments) in the barrel field were imaged with a Leica SP8 laser scanning confocal microscope equipped with HyD detectors for improved sensitivity. 50 µm dendritic segments were imaged with a 63X oil immersion objective (1.4 NA) at 1024x512 frame size, 4.1x digital zoom, and 0.1 µm Z-step size, generating a voxel size of 44 x 44 x 100 nm. DiI was excited using an OPSL 552 laser line with a pinhole of 0.8 Airy Units (AU). Laser power and gain were initially optimized, and then held relatively constant for the remainder of the experiment (i.e. laser power and gain were dynamically adjusted to avoid saturated voxels). Imaging parameters were chosen based off the Nyquist theorem as recommended by Huygens software (Scientific Volume Imaging, Hilversum, NL), which was used for deconvolution. Deconvolved images were imported into BitPlane Imaris (Version 9.1, Zurich, CH) for 3D reconstruction. The filament module was used to trace each dendrite, and the autopath tool was used to assign spines across each dendrite. Spine density per µm of dendrite and average spine head diameter of each dendritic segment were exported as variables.

Tamoxifen Treatment of *Mef2c cHet*^{Cx3Cr1} and *Cx3Cr1*$^{creER/+}$; Ai14 Mice: To induce recombination of the *Mef2c* floxed allele or Gt(ROSA)26Sor locus to express tdTomato in microglia, *Cx3Cr1*$^{creER/+}$, *Mef2c*$^{fl/+}$ (experimental) and *Cx3Cr1*$^{creER/+}$, *Mef2c*$^{+/+}$ (control) or *Cx3Cr1*$^{creER/+}$; Ai14 pups were treated with tamoxifen via mother's milk (100 mg/kg of tamoxifen in 10% ethanol/90% sesame oil i.p. injection of dam) from post-natal day 1 through post-natal day 3 . Starting at post-natal day 4, treated pups were then fostered by a lactating CD-1 female mouse until weaning. The tamoxifen administration protocol was adapted from (23).

Immunohistochemistry: Mice were terminally anesthetized with ketamine/xylazine and transcardially perfused with PBS followed by 4% (w/v) paraformaldehyde (PFA). Brains were post-fixed for >24 hours at 4°C in 4% PFA then cryoprotected in 30% sucrose. Brains were coronally sectioned at 40-50 µm using

a sliding microtome and stored in 1X PBS with 0.02% sodium azide. Anti-IBA1 IHC was performed based on manufacturer's protocol with modifications (Wako). Sections were washed 3 times for 10 minutes with 1 X PBS with TritonX-100 (0.3%). Sections were then blocked with 1X PBS with 1% BSA and 0.3% TritonX-100 for 2 hours. Sections were immunostained with primary rabbit anti-IBA1 antibody (1:1000; Wako 019-19741) overnight at 4°C followed by Cy3 conjugated goat anti-rabbit secondary antibody (1:400 for 2 hours) or Alexa-Fluor-647 donkey anti-rabbit secondary antibody (1:400 for 2 hours). Sections were mounted with Prolong Gold with DAPI mountant (ThermoFisher).

Anti-GFP and anti-MEF2C IHC was performed as described in the following. Sections were washed 3 times for 10 minutes with 1 X PBS with TritonX-100 (0.3%) and then blocked in 3% bovine serum albumin, 3% normal donkey serum, 0.3% triton X-100, 0.2% tween-20 in 1X PBS. Sections were immunostained with primary chicken anti-GFP (1:1000; Aves GFP-1020) antibody and rabbit anti-MEF2A/MEF2C (1:300; abcam ab197070) antibody overnight at 4°C followed by Alexa Fluor-488 donkey anti-chicken (1:400) and Cy3 donkey anti-rabbit secondary antibody (1:200) for 1.5 hours. Sections were mounted with Prolong Gold with DAPI mountant (ThermoFisher).

Confocal Imaging and Image Analysis: Iba1 stained sections were imaged on a Zeiss 880 confocal microscope at 20x objective. On average, 3 images were imaged per mouse/brain region. Images were deconvolved in AutoQuant (Bitplane) and analyzed in Imaris software (Bitplane). Imaris analysis began with surface rendering of Iba1+ cells. The mean intensity of each cell, cell number, and cell soma volume were calculated in the Imaris software. The mean intensity of each cell by animal was entered into GraphPad Prism software to generate cumulative frequency distributions. Statistical testing was performed on this data via Kolmogorov–Smirnov test. Iba1+ cell numbers per field and cell soma volumes were entered into GraphPad Prism by genotype and brain region. Genotype-based differences in Iba1+ cell numbers were assessed via unpaired two-tailed or nested t-tests. Imaging of MEF2C expression in microglia was performed on a Zeiss 880 confocal microscope at 40x objective. Imaging to confirm microglia-specific recombination was performed in *Cx3Cr1*$^{creER/+}$; Ai14 mice that express tdTomato under

the Gt(ROSA)26Sor locus. Stained sections were imaged on a Zeiss 880 confocal microscope at 20x objective. Quantification was performed in Fiji by counting.

RNAscope: Sixteen-micron brain tissue sections from mice at P35 were generated on a cryostat. RNAscope was performed targeting *Mef2c* (Advanced Cell Diagnostics #421011, mm-Mef2c, 1:2000) and *Cx3Cr1* (Advanced Cell Diagnostics #314221-C2, mm-Cx3cr1-C2, 1:2000) mRNA. The RNAscope was performed following the manufacturer's protocol for the RNAscope Multiplex Fluorescent Detection Reagents v2 kit (Advanced Cell Diagnostics #323110). The Mef2c-C1 probe was processed to fluorescein (PerkinElmer #FP1168) and the Cx3cr1-C2 probe was processed to cyanine 3 (PerkinElmer #FP1170) in RNAscope Multiplex TSA buffer (Advanced Cell Diagnostics #322809).

Cytokine Antibody Array: The cytokine antibody array (Proteome Profiler Mouse Cytokine Array Kit, Panel A, R&D Systems #ARY006) was performed according to manufacturer's instructions except the membranes were blocked for 2 hours. A starting concentration of 450 μg of cortical brain tissue from *Mef2c*-Het and controls were used for each membrane.

Supplemental References

1. Arnold MA, Kim Y, Czubryt MP, Phan D, McAnally J, Qi X, et al. (2007): MEF2C transcription factor controls chondrocyte hypertrophy and bone development. *Developmental cell*. 12:377-389.
2. Gorski JA, Talley T, Qiu M, Puelles L, Rubenstein JLR, Jones KR (2002): Cortical Excitatory Neurons and Glia, But Not GABAergic Neurons, Are Produced in the Emx1-Expressing Lineage. *The Journal of Neuroscience*. 22:6309-6314.
3. Barski JJ, Dethleffsen K, Meyer M (2000): Cre recombinase expression in cerebellar Purkinje cells. *Genesis*. 28:93-98.
4. Parkhurst CN, Yang G, Ninan I, Savas JN, Yates JR, 3rd, Lafaille JJ, et al. (2013): Microglia promote learning-dependent synapse formation through brain-derived neurotrophic factor. *Cell*. 155:1596-1609.
5. Pulipparacharuvil S, Renthal W, Hale CF, Taniguchi M, Xiao G, Kumar A, et al. (2008): Cocaine regulates MEF2 to control synaptic and behavioral plasticity. *Neuron*. 59:621-633.

6. Ey E, Torquet N, Le Sourd AM, Leblond CS, Boeckers TM, Faure P, et al. (2013): The Autism ProSAP1/Shank2 mouse model displays quantitative and structural abnormalities in ultrasonic vocalisations. *Behavioural brain research*. 256:677-689.

7. Harrington AJ, Raissi A, Rajkovich K, Berto S, Kumar J, Molinaro G, et al. (2016): MEF2C regulates cortical inhibitory and excitatory synapses and behaviors relevant to neurodevelopmental disorders. *Elife*. 5.

8. Scattoni ML, Gandhy SU, Ricceri L, Crawley JN (2008): Unusual repertoire of vocalizations in the BTBR T+tf/J mouse model of autism. *PloS one*. 3:e3067.

9. Wehner JM, Radcliffe RA (2004): Cued and contextual fear conditioning in mice. *Curr Protoc Neurosci*. Chapter 8:Unit 8 5C.

10. Rosenfeld CS, Ferguson SA (2014): Barnes maze testing strategies with small and large rodent models. *J Vis Exp*.e51194.

11. Renthal W, Maze I, Krishnan V, Covington HE, 3rd, Xiao G, Kumar A, et al. (2007): Histone deacetylase 5 epigenetically controls behavioral adaptations to chronic emotional stimuli. *Neuron*. 56:517-529.

12. Taniguchi M, Carreira MB, Cooper YA, Bobadilla AC, Heinsbroek JA, Koike N, et al. (2017): HDAC5 and Its Target Gene, Npas4, Function in the Nucleus Accumbens to Regulate Cocaine-Conditioned Behaviors. *Neuron*. 96:130-144 e136.

13. Dobin A, Davis CA, Schlesinger F, Drenkow J, Zaleski C, Jha S, et al. (2013): STAR: ultrafast universal RNA-seq aligner. *Bioinformatics*. 29:15-21.

14. Anders S, Pyl PT, Huber W (2015): HTSeq--a Python framework to work with high-throughput sequencing data. *Bioinformatics*. 31:166-169.

15. Chen J, Bardes EE, Aronow BJ, Jegga AG (2009): ToppGene Suite for gene list enrichment analysis and candidate gene prioritization. *Nucleic acids research*. 37:W305-311.

16. Telese F, Ma Q, Perez PM, Notani D, Oh S, Li W, et al. (2015): LRP8-Reelin-Regulated Neuronal Enhancer Signature Underlying Learning and Memory Formation. *Neuron*. 86:696-710.

17. Li H, Durbin R (2009): Fast and accurate short read alignment with Burrows-Wheeler transform. *Bioinformatics*. 25:1754-1760.

18. Li H, Handsaker B, Wysoker A, Fennell T, Ruan J, Homer N, et al. (2009): The Sequence Alignment/Map format and SAMtools. *Bioinformatics*. 25:2078-2079.

19. Kharchenko PV, Tolstorukov MY, Park PJ (2008): Design and analysis of ChIP-seq experiments for DNA-binding proteins. *Nat Biotechnol*. 26:1351-1359.

20. Zhang Y, Liu T, Meyer CA, Eeckhoute J, Johnson DS, Bernstein BE, et al. (2008): Model-based analysis of ChIP-Seq (MACS). *Genome biology*. 9:R137.

21. Yu G, Wang LG, He QY (2015): ChIPseeker: an R/Bioconductor package for ChIP peak annotation, comparison and visualization. *Bioinformatics*. 31:2382-2383.

22. Spencer S, Neuhofer D, Chioma VC, Garcia-Keller C, Schwartz DJ, Allen N, et al. (2018): A Model of Delta(9)-Tetrahydrocannabinol Self-administration and Reinstatement That Alters Synaptic Plasticity in Nucleus Accumbens. *Biol Psychiatry*. 84:601-610.

23. Agarwal A, Dibaj P, Kassmann CM, Goebbels S, Nave K-A, Schwab MH (2012): In vivo imaging and noninvasive ablation of pyramidal neurons in adult NEX-CreERT2 mice. *Cereb Cortex*. 22:1473-1486.